

Remote Sensing of Heart Rate and Patterns of Respiration on a Stationary Subject Using 94 GHz Millimeter Wave Interferometry

Ilya V. Mikhelson, *Student Member, IEEE*, Sasan Bakhtiari, *Senior Member, IEEE*,
Thomas W. Elmer II, *Member, IEEE*, and Alan V. Sahakian*, *Fellow, IEEE*

Abstract—Using continuous wave, 94 GHz millimeter-wave interferometry, a signal representing chest wall motion can be obtained that contains both the heart rate and respiration patterns of a human subject. These components have to be separated from each other in the received signal. Our method was to use the quadrature and in-phase components of the signal, after removing the mean of each, to find the phase, unwrap it, and convert it to a displacement measurement. Using this, the power spectrum was examined for peaks, which corresponded to the heart rate and respiration rate. The displacement waveform of the chest was also analyzed for discrete heartbeats using a novel wavelet decomposition technique.

Index Terms—Millimeter-wave, Non-contact, Cardiography, Respiration, Heart rate.

I. INTRODUCTION

THE reasons to gather physiological parameters at a distance range from medical monitoring, to security, to military use. There is a growing need for non-contact medical monitoring equipment, for observing individuals unobtrusively at home. It has been shown that this kind of equipment can be used for respiratory monitoring while a subject sleeps [1]. It has also been used to detect whether a person is lying without the subject even knowing he was being tested, by observing his vital signs as he answers questions [2]. Furthermore, this form of technology has been used to determine if people are alive in situations where it may be dangerous to try to retrieve a person [3].

The goal of this project is to remotely obtain human physiological parameters, specifically heart rate and respiration rate, using millimeter-wave interferometry. What separates this from past research is the fact that we use a higher frequency for much finer displacement resolution, which could allow observing not simply the rate of heartbeats, but even details in the heartbeat pattern. Additionally, the higher frequency of

operation creates a smaller beam divergence with a practically-sized antenna, thus allowing accurate measurements to be taken from greater distances.

There is prior work in remote detection of vital signs. In 1975, it was shown that the respiratory rate could be obtained from a clothed subject from 0.3 m away using microwaves and the Doppler effect [4]. It was also shown in the late 1970s that the heart rate could be remotely obtained as well [5]. This was based upon the fact that the chest moves periodically with respiration and with heartbeat. Using the fact that radio frequency (RF) waves undergo a small frequency shift when reflected from a moving surface such as the chest, the heart rate and respiratory rate can be extracted using signal processing.

Detection of heart rate and respiration has been reported using several frequency ranges such as 2.4 GHz [6], 10 GHz [7], and 60 GHz [8]. In these studies, the phase was extracted from an in-phase and quadrature component and was used to compute the displacement of the chest. Our system employs a higher frequency (94 GHz) to resolve smaller displacement. This is important because chest wall motion due to heart beats is about 0.5 mm, while that due to respiration varies from 4 mm to 12 mm [9].

There have also been tests done with a 228 GHz system [10]. This system, however, requires a lot of specialized instrumentation to operate at such a high frequency. Even though such a system would naturally obtain higher displacement resolution, we chose to stay at a lower frequency because one of our goals was to make an economical and practical solution.

We also looked at the pattern of chest motion due to the beating of the heart while respiration was suppressed. This has been done in the past using motion sensors attached to the body [11] – [13]. The authors called this the kinetocardiogram, which was simply the outward displacement of the chest. The biggest problem at the time was that these sensors created interference of their own because they were attached to the subject. Therefore, the authors suggested that the best way to get this data would be to use some form of non-contact technique. At the time this was unavailable, but now we can do just that. In fact, the displacement resolution we observe is fine enough to be able to potentially see intricacies in the heart beat waveform that could be used for medical diagnoses without having to touch the patient at all.

Another method that has been used in the past to try to separate heartbeats and respiration has been to use wavelets

Manuscript received September 3, 2010; revised December 14, 2010. This work was supported in part by the U.S. Department of Energy.

I. V. Mikhelson is with the Department of Electrical Engineering and Computer Science, Northwestern University, Evanston, IL 60208 USA (e-mail: i-mikhelson@u.northwestern.edu).

S. Bakhtiari and T. W. Elmer are with the Nuclear Engineering Division, Argonne National Laboratory, Argonne, IL 60439 USA (e-mail: bakhtiari@anl.gov; elmer@anl.gov).

*A. V. Sahakian is with the Department of Electrical Engineering and Computer Science and the Department of Biomedical Engineering, Northwestern University, Evanston, IL 60208 USA (e-mail: sahakian@eecs.northwestern.edu).

[14]. A wavelet decomposition allows for high frequency resolution at low frequencies and for high time resolution at high frequencies [15]. This is a good property when looking at a signal with heart rate and respiration, since the high frequency heartbeats are quick events, while low frequency breathing is a slow event.

This paper will demonstrate a method to find heart rate through a proof of concept of the techniques. The conditions for the tests are ideal, as the tests are used to validate the algorithms.

II. METHODS

We constructed a 94 GHz continuous-wave (CW) millimeter-wave interferometer for displacement signal acquisition, adapted from [16]. A diagram of the setup is shown in Fig. 1. In the setup, a CW 94 GHz signal is generated by a cavity tuned Gunn diode oscillator. It is then transmitted at a target using a Gaussian (quasi-optical) antenna with a 15.24 cm lens, resulting in the far-field starting at approximately 1.8 meters and a beam divergence of approximately 1.5 degrees. The antenna itself is shown in Fig. 2. There is an optical telescope on top of the antenna for accurate aiming.

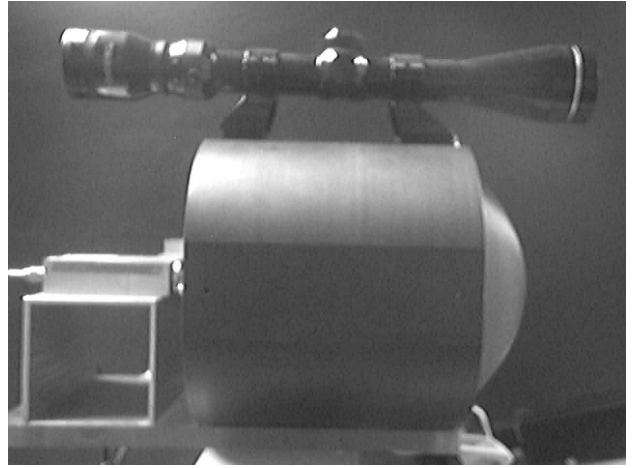


Fig. 2. Setup of antenna.

The displacement is clearly modulated on the phase of the signal. To isolate the phase, we used:

$$phase = \arctan\left(\frac{Q}{I}\right). \quad (4)$$

After this, the displacement could be easily calculated to be the phase scaled by an appropriate factor:

$$\begin{aligned} d &= \frac{c}{2\omega_0} \arctan\left(\frac{Q}{I}\right) \\ &= \frac{\lambda_0}{4\pi} \arctan\left(\frac{Q}{I}\right), \end{aligned} \quad (5)$$

where

$$\lambda_0 = \frac{2\pi c}{\omega_0}.$$

When the signal is reflected off a human target, there are several vector components embedded in the relative magnitude and phase of the returned signal. There is a small rotating vector defined by equations (2) and (3), which is what we were interested in extracting, because it represents the small displacements of the chest wall due to respiration and cardiac activity. There is also a series of much larger vectors added to the small rotating vector, which is due to reflections from any number of things, from walls to other people moving. A visualization of this can be seen in Fig. 3. The bigger vectors are all lumped into the large white vector, which for our experiments is assumed to be stationary. To find displacement of the chest, we isolated just the small black vector and eliminated the rest.

A very important factor in our study is the high frequency we used. At 94 GHz, the free-space wavelength λ_0 is 3.19 mm, meaning that a target displacement of 1.595 mm will cause a full rotation of the rotating vector we are trying to isolate. At this scale, we have very fine resolution of motions of the chest making heartbeats easily resolvable. To interpret the data correctly, however, the phase that was found with the aforementioned method must be unwrapped due to the 2π periodicity of phase.

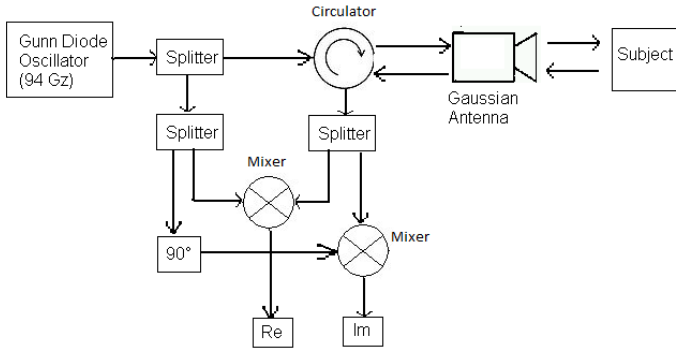


Fig. 1. Millimeter-wave interferometer setup.

Using several simplifying assumptions, the reflected signal ($r(t)$) is defined as:

$$\begin{aligned} r(t) &= \cos\left(\omega_0\left(t - \frac{2d}{c}\right)\right) \\ &= \cos\left(\omega_0 t - \frac{2\omega_0 d}{c}\right), \end{aligned} \quad (1)$$

where d is the displacement, c is the speed of light, and ω_0 is the angular frequency $94 * 2\pi * 10^9$ rads/sec. This is then mixed with a sample of the transmitted signal as shown in Fig. 1 and low-pass filtered to create an in-phase (I) and a quadrature (Q) component of the net reflection:

$$I = \frac{1}{2} \cos\left(\frac{2\omega_0 d}{c}\right), \quad (2)$$

$$Q = \frac{1}{2} \sin\left(\frac{2\omega_0 d}{c}\right). \quad (3)$$

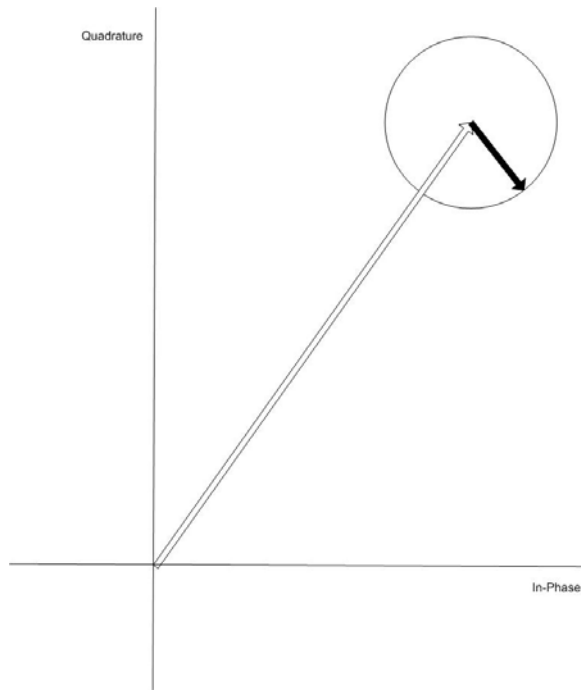


Fig. 3. State space visualization.

It should also be mentioned that any of the motion that is detected with our system is due to the movements of the surface of the chest. This can be verified by finding that the skin depth of human skin at 94 GHz is 0.37 mm [17]. Since the average human dermal thickness is between 2 mm and 3 mm [18], most of the power is attenuated long before the wave penetrates the skin, and thus everything we see is due to the motion of the skin.

At 94 GHz, the beam is able to penetrate optically opaque materials, such as clothing, and reflect off skin [16]. Naturally, if a person is wearing something made of metal in the area that the antenna is aiming at, there would be a problem. However, with a lens radius of 15.24 cm, there is a good chance that the reflection will still contain some usable data. Another good property of this frequency is that it is near a local minimum in terms of atmospheric attenuation [19]. Since this device is meant for indoor data acquisition, this frequency is a good choice.

With this setup, we recorded data for a clothed subject ten meters away. The subject was wearing a tee-shirt, and the data acquisition took place indoors. We used an NI PCI-4474 24-bit DAQ and LabView's data acquisition software. Each recorded interval was 8.192 seconds of data (for easy FFT processing), sampled at 1000 Hz. We then processed this data using a customized program written in MATLAB, utilizing MATLAB's signal processing toolbox.

To find the displacement of the chest wall, we started by trying to eliminate the vectors that were not due to chest motion. This was done by subtracting the mean of the in-phase part of the signal from itself, and likewise for the quadrature part. This created a zero-mean signal in which the only vector left was the one rotating around the origin due to the chest displacement, as can be seen in Fig. 4. Then, we

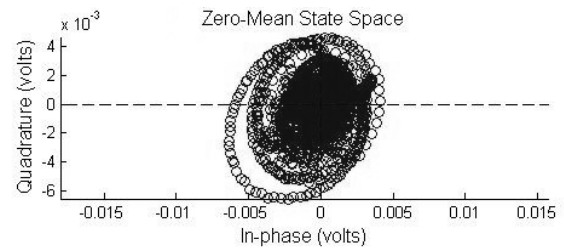


Fig. 4. State space after shifting the mean to the origin.

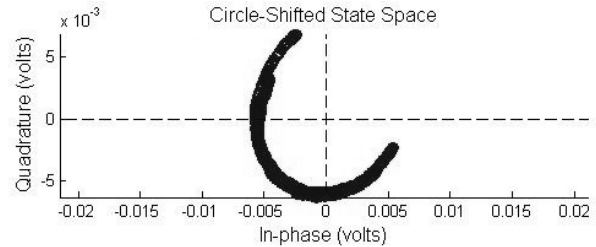


Fig. 5. State space after shifting the center of the best fit circle to the origin.

found the phase and calculated the displacement as described earlier. Since we wanted a continuous graph of displacement, we used an unwrapping algorithm to eliminate the inherent discontinuities at $\pm\pi$ due to the periodicity of phase.

Since the displacement of the chest due to respiration causes several rotations of the vector in the state space, taking a mean of the data and subtracting it is viable. However, when there is no respiration, for example when we want to closely examine the heart pattern, only an arc of the rotating vector will be traced out. In this case, the mean would not be a good estimate of the center of the rotating vector. For this case, we fitted a circle to the data, and subtracted the center of the best fit from the data to move it to the origin, as seen in Fig. 5. It is clear that fitting a circle is a better solution.

For this kind of experiment, we took measurements from 2 to 9 meters away. We fed the data into an NI USB-9239 24-bit analog input module, using a sampling rate of 5000 Hz. We then processed the data in MATLAB. We first low-pass filtered the data at 1000 Hz using a sixth-order Butterworth filter, and then fitted a circle to the data and moved the data so that the center of the circle would be at the origin. Then, we found the phase as before, using the arctangent. At the same time as gathering this data, an ECG was also gathered from the subject to use as a gold standard to examine the accuracy of heartbeat detection. This was done using a Tektronix 408 ECG monitor, and feeding the ECG into an NI USB-6212 16-bit M Series MIO DAQ.

The displacement data was then processed using a wavelet decomposition technique. A sample signal is shown in Fig. 6. This is the calculated displacement recorded from 3 m while the subject was breathing normally. First, the data was decimated by 100 to make the sampling rate 50 Hz instead of the initial 5000 Hz. Then, using a symlet 32 wavelet, we performed a one-level multi-resolution analysis, yielding two signals: a high-pass filtered one and a low-pass filtered one. The high-pass filtered signal had a waveform as shown in Fig.

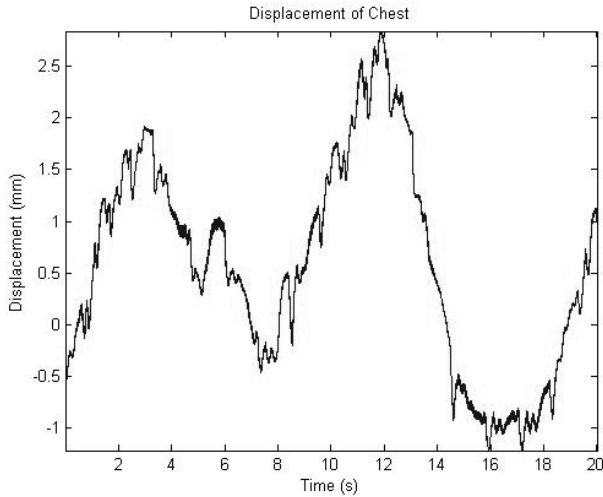


Fig. 6. Displacement of chest from 3 m with breathing.

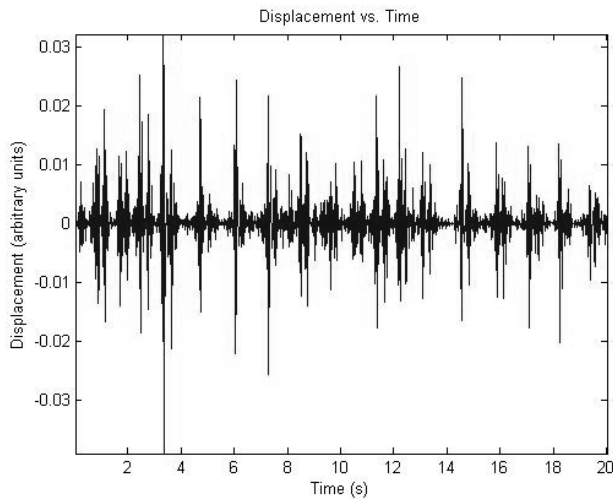


Fig. 7. High-pass filtered result of one level multi-resolution analysis.

7. It was clear that there were higher amplitude oscillations associated with heartbeats. Therefore, we took the absolute value of that signal, and used a moving average filter of length 20 on it. This created the signal shown in Fig. 8. It is clear here that there are distinct peaks corresponding to the heartbeats, so we simply found the peaks of this signal, and designated those as the heartbeats.

The ECG data was also used to remove the baseline wander from data collected with the millimeter-wave sensor. This was done by using the Pan-Tompkins algorithm [20] to find the QRS complexes in the ECG, and fitting a spline to the collected displacement data at the points found using that algorithm. Then, the spline fit was subtracted from the collected displacement signal. The data without baseline wander gave a better representation of the chest displacement. However, it is important to note that the aforementioned processing was performed without baseline wander removal. The baseline wander was removed for display purposes, to show that the obtained signal closely matches the ECG and the signals found

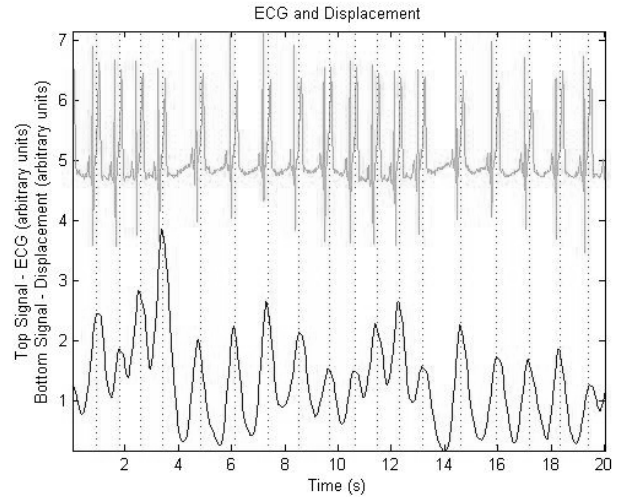


Fig. 8. Waveform after finding absolute value and applying moving average filter, with superimposed ECG and vertical lines corresponding to heartbeats in the ECG.

using the kinetocardiogram in [11] – [13].

III. RESULTS AND DISCUSSION

We began our testing with a simulation of chest movement due to cardiac and respiratory activity by using a shaker combined with a function generator. The shaker was a vibration exciter (Vibration Exciter Type 4809 from Brüel & Kjær) whose motion was controlled by the function generator. This allowed us to simulate the movement of the chest wall in order to demonstrate the proof-of-concept.

First, we used a reading from a laser vibrometer which was a “perfect” recreation of what we were trying to achieve. Fig. 9 shows the waveform as gathered from the shaker and function generator setup described earlier. We then used our interferometer configuration on the same setup. Figs. 10(a), 10(b) show the data the interferometer gathered from the shaker and function generator, and Fig. 10(c) shows the unwrapped phase converted to a measure of displacement using our technique. The displacement is very close to the laser vibrometer signal, which is a gold standard against which we measured. This proved that the phase unwrapping algorithm worked.

Using this routine, we tried to obtain the heart rate and respiratory rate from an actual human subject breathing steadily and standing still against a wall. Figs. 11(a), 11(b) show the reflected signal that contains both heart rate and respiration. It should be noted that whereas in Figs. 10(a) and 10(b) the separate beats due to the shaker are evident, no such thing can be said about the waveforms in Figs. 11(a) and 11(b). We again applied the same algorithm as before, and generated the results seen in Fig. 11(c). Next, we obtained a power spectrum for the unwrapped signal which is shown in Fig. 12. From the power spectrum, which is plotted on a decibel scale on the y-axis, it is possible to read the heart rate and the respiration rate. The respiration rate corresponds to a peak around 0.2-0.6 Hz, and the heart rate corresponds to a peak around 0.8-1.5 Hz. This is the range of values that would be expected for a calm adult human.

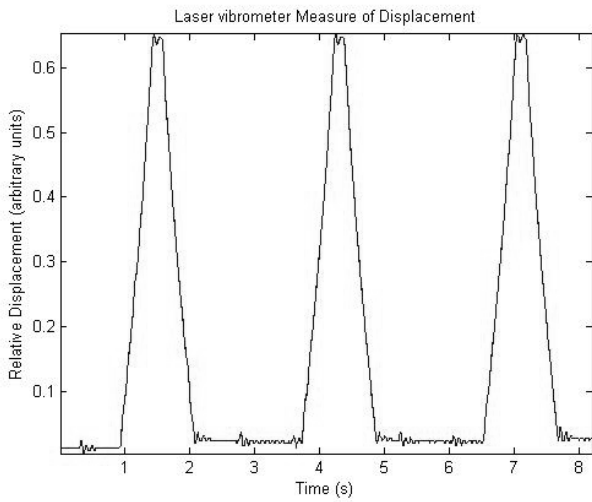


Fig. 9. Laser vibrometer displacement waveform.

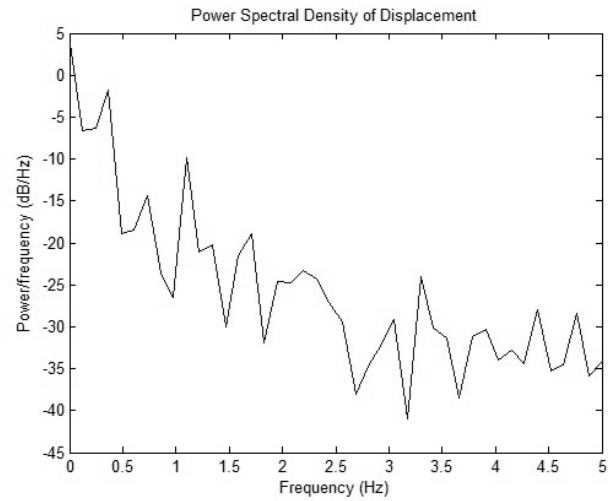


Fig. 12. Power spectrum of chest displacement.

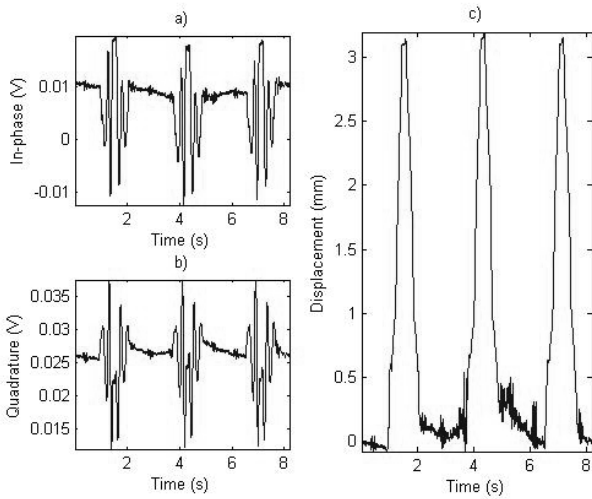


Fig. 10. a) In-phase shaker and function generator signal, b) Quadrature shaker and function generator signal, and c) Calculated displacement of shaker.

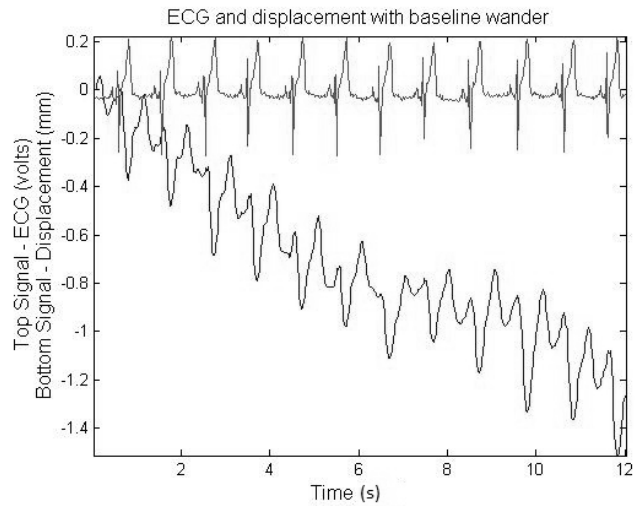


Fig. 13. Chest displacement and ECG while holding breath.

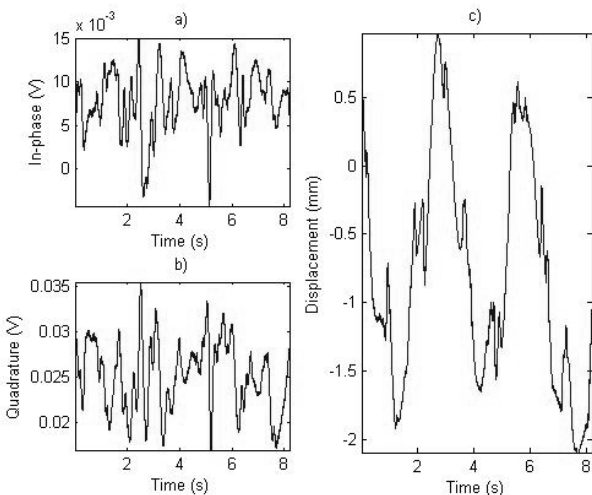


Fig. 11. a) In-phase signal from human, b) Quadrature signal from human, and c) Calculated displacement of signal from human.

When breathing was suppressed, we found a result similar to the kinetocardiograms observed in [11] – [13]. Both the ECG and the resultant displacement waveform can be seen in Fig. 13. The signal after baseline removal can be seen in Fig. 14. It is clear that the displacement signal is due to the heart beating, since the waveform aligns with events in the ECG.

To test the wavelet decomposition technique, we gathered data from several distances and under the conditions of breathing and not breathing. The subject was wearing a tee-shirt in each sample, and samples were taken at 1 meter increments from 2 meters to 9 meters from the antenna. In each sample, the subject was seated with back support and was facing the antenna, which was aimed at the center of the chest around the level of V2 in an ECG. The results were good in most cases, with a couple of samples presented here. The results from using the wavelet technique on data gathered from 5 meters with breathing can be seen in Fig. 15. This shows the estimated heartbeats superimposed on the actual displacement waveform, and the ECG with the estimated heartbeats. The

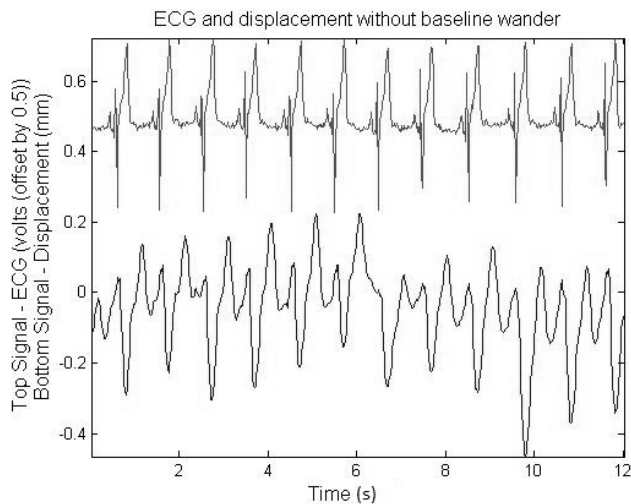


Fig. 14. Chest displacement and ECG while holding breath, with baseline wander removed.

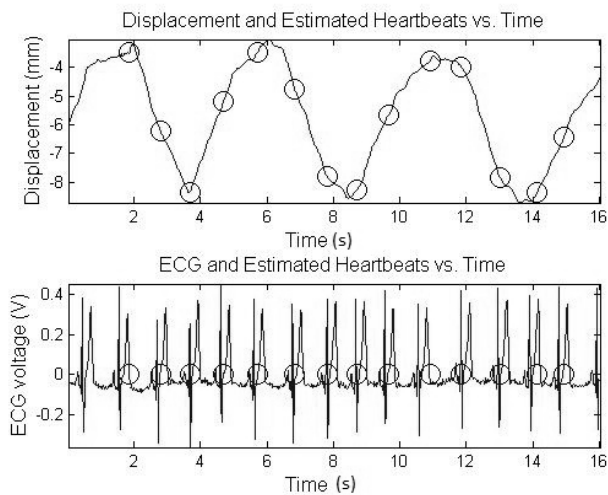


Fig. 15. Displacement waveform and ECG with heartbeats superimposed, gathered at 5 meters with breathing.

heart rate estimated by the wavelet method was 59.6 bpm. This was obtained by finding the average spacing in between estimated heartbeats. The true heart rate, obtained by dividing the number of QRS complexes by the amount of time of the data sample, was 59.9 bpm. Another sample, gathered at 9 meters with breathing suppressed, can be seen in Fig. 16. Again, the accuracy of the estimation method can easily be seen, as the estimated heart rate was 65.9 bpm, whereas the actual heart rate, calculated by the same method as before, was 65.9 bpm.

IV. CONCLUSION

The millimeter-wave interferometer reliably split the reflected signal into its in-phase and quadrature components. The technique of subtracting means (or a circle center) and unwrapping the phase, which can easily be converted to a measure of displacement, appeared to work effectively for separating the heart rate and respiration rate from a signal

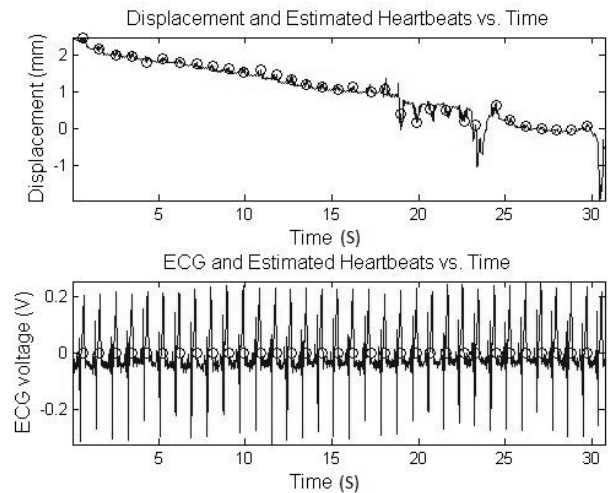


Fig. 16. Displacement waveform and ECG with heartbeats superimposed, gathered at 9 meters with no breathing.

that contained both. This method provided promising results as it gave accurate measurements for both the heart rate and respiratory rate in several trials from up to ten meters away.

When breathing was suppressed, the remaining waveform was clearly due to the cardiac cycle, and contained a great amount of detail. Future work will focus on extracting this same level of detail from a subject breathing normally. Also, since this whole study was performed under ideal conditions, further work will have to be done to find a way to extract data in non-ideal conditions, such as those involving subject movement and ambient motion.

Finally, the wavelet decomposition technique gave an accurate representation of the location of heartbeats, even in data where the heartbeats were not clearly visible or easy to detect. Future work will focus on finding an optimal wavelet for this specific task.

REFERENCES

- [1] M. Uenoyama, T. Matsui, K. Yamada, S. Suzuki, B. Takase, S. Suzuki, M. Ishihara, and M. Kawakami, "Non-contact respiratory monitoring system using a ceiling-attached microwave antenna," *Med. Bio. Eng. Comput.*, vol. 44, pp. 835–840, Aug. 2006.
- [2] J. Geisheimer and D. F. Greneker, III, "A non-contact lie detector using radar vital signs monitor (RVSM) technology," *IEEE Aerosp. Electron. Syst. Mag.*, vol. 16, no. 8, pp. 10–14, Aug. 2001.
- [3] V. M. Lubecke, O. Boric-Lubecke, A. Host-Madsen, and A. E. Fathy, "Through-the-wall radar life detection and monitoring," in *Proc. IEEE MTT-S Int. Microw. Symp.*, Honolulu, HI, Jun. 2007, pp. 769–772.
- [4] J. C. Lin, "Non-invasive microwave measurement of respiration," *Proc. IEEE*, vol. 63, pp. 1530, 1975.
- [5] B. Lohman, O. Boric-Lubecke, V. M. Lubecke, P. W. Ong, and M. M. Sondhi, "A Digital Signal Processor for Doppler Radar Sensing of Vital Signs," *IEEE Eng. in Med. and Bio. Mag.*, vol. 21, no. 5, pp. 161–164, Sept. 2002.
- [6] D. R. Morgan, M. G. Zierdt, "Novel signal processing techniques for Doppler radar cardiopulmonary sensing," *Signal Process.*, vol. 89, pp. 45–66, 2009.
- [7] O. Boric-Lubecke, P. W. Ong, V. M. Lubecke, "10 GHz Doppler sensing of respiration and heart movement," in *Proc. IEEE 28th Annual Northeast Bioeng. Conf.*, Philadelphia, PA, Apr. 2002, pp. 55–56.
- [8] D. Obeid, S. Sadek, G. Zaharia, and G. El-Zein, "Non-contact heartbeat detection at 2.4, 5.8 and 60 GHz: A comparative study," *Microwave Opt. Technol. Lett.*, vol. 51, no. 3, pp. 666–669, Mar. 2009.

- [9] A. D. Droitcour, "Non-contact measurement of heart and respiration rates with a single-chip microwave Doppler radar," Ph.D. dissertation, Dept. Elect. Eng., Stanford University, Palo Alto, CA, 2006.
- [10] D. T. Petkie, C. Benton, E. Bryan, "Millimeter wave radar for remote measurement of vital signs," *Radar Conference, 2009 IEEE*, Pasadena, CA, May 2009, pp. 1–3.
- [11] E. E. Eddleman, Jr., K. Willis, T. J. Reeves, and T. R. Harrison, "The kinetocardiogram: I. Method of recording precordial movements," *Circulation*, vol. 8, pp. 269–275, 1953.
- [12] E. E. Eddleman, Jr., K. Willis, L. Christianson, J. R. Pierce, and R. P. Walker, "The kinetocardiogram: II. The normal configuration and amplitude," *Circulation*, vol. 8, pp. 370–380, 1953.
- [13] E. E. Eddleman, Jr., K. Willis, "The kinetocardiogram: III. The distribution of forces over the anterior chest," *Circulation*, vol. 8, pp. 569–577, 1953.
- [14] W. Jianqi, Z. Chongxun, L. Guohua, and J. Xijing, "A new method for identifying the life parameters via radar," *EURASIP Journal on Advances in Signal Processing*, vol. 2007, issue 1, pp. 16, Jan. 2007.
- [15] O. Rioul and M. Vetterli, "Wavelets and signal processing," *IEEE Signal Processing Mag.*, vol. 8, pp. 14–38, Oct. 1991.
- [16] S. Bakhtiari, N. Gopalsami, T. W. Elmer, and A. C. Raptis, "Millimeter wave sensor for far-field standoff vibrometry," in *Proc. AIP Conf.*, vol. 1096, pp. 1641–1648, 2009.
- [17] D. Andreuccetti, R. Fossi, and C. Petrucci. (2007). Dielectric properties of body tissues. Institute of Applied Physics - CNR. Florence, Italy. [Online]. Available: <http://niremf.ifac.cnr.it/tissprop/>.
- [18] S. Kusuma, R. K. Vuthoori, M. Piliang, and J. E. Zins, "Skin anatomy and Physiology," in *Plastic and Reconstructive Surgery* (Springer Specialist Surgery Series, Part III), M. Z. Siemionow and M. Eisenmann-Klein, Eds. London, England: Springer London, 2010, ch. 13, pp. 161–171.
- [19] J. M. Golio, *RF and microwave passive and active technologies*, CRC Press, 2008.
- [20] J. Pan, W. J. Tompkins, "A real-time QRS detection algorithm," *IEEE Trans. Biomed. Eng.*, vol. 32, no. 3, pp. 230–236, Mar. 1985.



Thomas W. Elmer II (M'07) received the B.S. degree in physics (with minors in math and computer science) from La Sierra University, Riverside, CA, in 1998, and the M.S. degree from the University of Illinois at Chicago, in 2004.

While with La Sierra University, he was with the Physics Department, where he was involved with writing and maintaining programs to run laboratory experiments. He has also lectured on astronomy and gravitational physics for the Physics Department.

His senior research project was with the Health Physics Department, Loma Linda University Medical Center, for which he analyzed the activation of Cerrobend(R) metal by 250-MeV protons at the hospitals Proton Facility. In 1999, he joined Argonne National Laboratory, Argonne, IL, as a Student Intern, eventually remaining as a Software Engineering Associate for the System Technologies and Diagnostics Department, Nuclear Engineering Division. He writes programming for modeling, motion control, data acquisition, and data analysis in the microwave, millimeter-wave, and terahertz sensors laboratories.

Mr. Elmer was the recipient of the 2007 Research and Development (R&D) 100 Award presented by R&D Magazine.



Ilya V. Mikhelson (S'08) received the B.S. degree in electrical engineering from Northwestern University, Evanston, IL, in 2009.

He is currently a graduate student working toward the Ph.D. degree in electrical engineering at Northwestern University. His research interests include digital signal processing, computer vision, and remote patient monitoring.



Sasan Bakhtiari (M'91-SM'94) received the B.S.E.E. degree from the Illinois Institute of Technology, Chicago, in 1983, the M.S.E.E. from the University of Kansas, Lawrence, in 1987, and the Ph.D. degree in electrical engineering from Colorado State University, Fort Collins, in 1992.

From 1984 to 1987, he was with the Radar Systems and Remote Sensing Laboratory, University of Kansas. From 1998 to 1992, he was with the Microwave Nondestructive Testing Laboratory, Colorado State University. In 1993, he joined Ar-

gonne National Laboratory, Argonne, IL, where he is currently an Electrical Engineer with the System Technologies and Diagnostics Department, Nuclear Engineering Division. He is also the Section Manager for the Nondestructive Evaluation (NDE) Section. He has authored or coauthored numerous technical publications in the areas of sensors and NDE.



Alan V. Sahakian (S'84-M'84-SM'94-F'07) received the Ph.D. degree in electrical engineering from the University of Wisconsin, Madison, in 1984.

In 1984, he joined Northwestern University, Evanston, IL, where he is currently a Professor of Electrical Engineering and Computer Science and Biomedical Engineering, and is also a Member of the Associate Professional Staff of Evanston Hospital. His past research has been concerned with problems of aviation systems reliability and

microwave/millimeter-wave communications and imaging systems. His current research interests include cardiac electrophysiology and automatic diagnosis and treatment of the atrial cardiac arrhythmias by implantable devices. He is the author or coauthor of more than 150 papers, abstracts, and book sections.

Dr. Sahakian has served as the Vice President for Publications and Technical Activities for the Engineering in Medicine and Biology Society (EMBS).